A Computational Environment to Simulate Complex Tendinous Topologies

F. J. Valero-Cuevas and H. Lipson
Sibley School of Mechanical and Aerospace Engineering, Cornell University, NY, USA

Abstract— **Static and dynamic manipulation of objects with the fingertips (precision pinch) is essential to the activities of daily living. Despite numerous efforts to study the hand and its pinch function [5, 18], a comprehensive understanding of biomechanical function and neuromuscular control of the fingers eludes researchers. To make progress in understanding precision pinch we are creating biomechanical models to simulate finger function, neuromuscular control and rehabilitation. An important challenge in creating biomechanical models of the fingers is to simulate the tension distribution in the extensor mechanism—a defining biomechanical feature of the fingers consisting of a tendinous network that wraps over the dorsum of the phalanges. We have created a biomechanical modeling environment that can, among other things, predict tension distribution in the extensor mechanism. Our predictions show that the distribution of tension can be very sensitive to the assumed network topology—the number of elements and their connectivity.**

Keywords— **Hand, thumb, motor control, relaxation algorithm**

I. Introduction

The neuro-musculo-skeletal elements of the human hand are notoriously complex, making it challenging for even the most experienced clinicians to understand and predict how pathology and treatment affect precision pinch. Aging, injury, and neurologic/orthopedic diseases impair manipulation in millions of people by disrupting the collaborative interactions among the numerous multi-articular muscles of the digits.

To understand the impairment and restoration of manipulation, we have begun by first comprehending the biomechanical requirements for static and dynamic precision pinch, and how the neuro-musculo-skeletal system meets those requirements. By "static precision pinch" we mean the sensorimotor ability to regulate the magnitude and direction of the fingertip force/torque vectors in the absence of finger motion. "Dynamic precision pinch" requires, in addition, the regulation of finger motion [10, 12]. For simplicity I use "finger" to mean any digit—including the thumb—unless otherwise specified, and "fingertip" as the portion of the tissue surrounding the distal phalanx in contact with the object manipulated. Studying precision pinch is a first step towards addressing general multi-finger manipulation, neural and anatomical coupling among digits [5, 6, 15] and free finger motion [2, 3, 11]. With this long-term objective in mind, we have worked to create realistic 3D biomechanical models of finger motion and force production. Meeting this engineering challenge will be instrumental to quantifying, explaining and predicting clinical outcomes of manipulation impairment. Here we present some of our work related to modeling the extensor mechanism of the fingers—a defining biomechanical feature of the fingers consisting of a tendinous network that wraps over the dorsum of the phalanges.

II. Methods

We have created a biomechanical computational environment that can predict tensions in the individual components of arbitrary tendinous networks as they wrap over anatomical structures in 3D. This is the first computational substrate that allows the description and simulation of complex 3D tendon networks, like the extensor mechanism of the fingers, which contain complex tendinous interconnections wrapping over bones, other tendons, and other anatomical structures.

A. Computational Environment

We have developed a computational environment to describe the structure of arbitrary topological arrangements of fundamental musculoskeletal building blocks (tendons, muscles, articular surfaces, bones, ligaments and pulleys). Each building block is defined by its parameter values and described by a strain-stress relationship (which can be highly nonlinear) and a function that relates strain to geometry (e.g. constant volume muscle). The model space allows us to construct models either interactively (through the graphical user interface), through a model description script (see text box), or through an application program interface, which allows external programs, such as a computational synthesis algorithm, to describe and solve models automatically. For example, we interactively constructed a topologically complex models of the extensor mechanism of the index finger in a matter of minutes (see Figure). Creating ball-and-socket, saddle-shaped, hinge and sliding joints is similarly done by defining joint axes or the

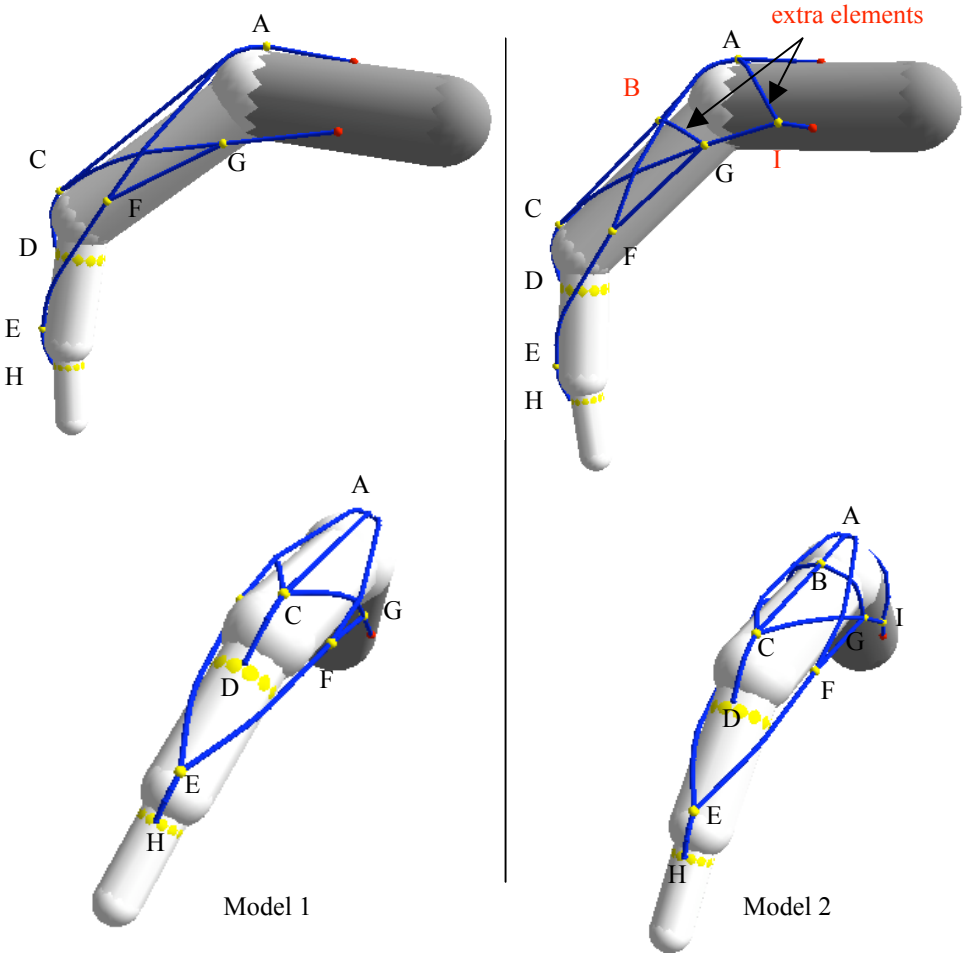
```
% JOINT X Y Z R /GROUNDED
J1 = JOINT 0.00 0.00 0.00 2.00
J2 = JOINT -40.00 -40.00 -40.00 2.00
J3 = JOINT 34.97 34.97 34.97 2.00 /GROUNDED
…
J46 = JOINT 6.99 6.99 6.99 0.50 /GROUNDED
J47 = JOINT 35.15 35.15 35.15 2.00 /GROUNDED
% LINK J1 J2 L K R
J1 = BONE J1 J2 40.00 1e+009 2.00
…
J8 = MUSCLE J8 J15 60.00 1e+009 2.00
J9 = TENDON J12 J21 17.11 1e+009 0.50
J10 = TENDON J16 J43 31.51 1e+009 0.50
J11 = PULLEY J14 J16 5.38 1e+009 0.50
…
```

geometry of the articular surfaces and adding ligaments with the appropriate origin and insertion points.

B. Relaxation Algorithm

In this modeling environment, the biomechanical function of the extensor mechanism emerges from the topological layout, size, and connectivity among viscoelastic elements. The biomechanical models are functional in the strict sense that we can predict (i) the new equilibrium 3D posture the digit will assume for a given change in muscle lengths if allowed to move; or (ii) the end-point, joint, and tendon forces for a given change in muscle force if constrained not to move. The model is a forward simulation process that uses a relaxation algorithm similar to that used for design automation of robotic neuro-musculo-skeletal structures [7, 8]. In response to a change in muscle force or length, the algorithm performs iterations until equilibrium is reached. Each iteration comprises two stages: computation of loads on all elements, and then computation of displacements at nodes needed to reach local equilibrium. The force-computation stage looks at each element of the structure and uses user-defined element-specific mathematical model to compute residual forces in that element at its current state. For example, if the element is a bone, a linear elastic model can be used with appropriate elastic coefficients. A tendon might behave elastically if it is in a state of tension, but might exert no force if in compression. Muscles might behave in more complex ways depending on their current activation signal and load, requiring a more elaborate model (such as activation-dependent viscoelasticity). In the second stage, all loads are accumulated at each of the structure nodes, and node displacements are calculated using node-specific mathematical models. For example, a node representing a ball-joint might move freely in the direction of the resultant force being applied to it. The exact amount of displacement can be estimated from the stiffness of the node, derived from the stiffness of the elements connected to it. A hinge joint might move in only one plane defined by the links connected to it. A grounded point will not move at all; a sliding node at the end of a tendon-pulley can move only along that tendon, and a node representing an insertion-point can move only to stay collinear with bone endpoints. Each node might then be displaced by the full calculated displacement, or by a fraction of it as a conservative measure (under-relaxation). These cycles are iterated until the residual force at any node is below a user-defined threshold (set to 0.25 N). The relaxation process resolves local equilibria, and by propagating loads and displacements global equilibrium is reached. If elements are well behaved (i.e. smaller displacements produce smaller loads, and conversely smaller loads produce smaller displacements), then the model will reach equilibrium after a finite number of steps. However, there might be more than one equilibrium configuration. The model will find the equilibrium state that can be reached through successive incremental adaptations from the initial configuration.

Although slower in our experience, the use of a relaxation solver over finite-element solvers allows for several benefits, specifically: (i) a relaxation solver is more accurate, as it takes into account angular changes at joints. This aspect is critical for correct musculoskeletal simulation as it involves large deformations and angular variations; (ii) a relaxation solver accommodates highly nonlinear behaviors, typical of biomechanical tissue (e.g. a tendon is nonlinearly elastic in tension but sustains no load in compression). And (iii) a relaxation solver is robust in



handling singularities in the model (e.g. tendon bifurcations or junctions in the extensor mechanism) and other model instabilities. Importantly, the fact that the simulator considers quasi-static viscous-like motion, and not true dynamic effects, is well suited to the simulation of everyday multi-digit manipulation. Numerous studies have established that the digits are damped systems where inertial effects are only important for high-speed trilling motions or tremor not seen in every-day manipulation tasks (e.g., [2, 9]). To our knowledge, this is the first computational environment that allows the automatic descriptions and simulation of biomechanical models that accommodate complex tendinous interconnections, such as those in the extensor mechanism that change with finger posture and tendon tensions [1, 4].

C. Simulating Two Alternative Tendinous Networks

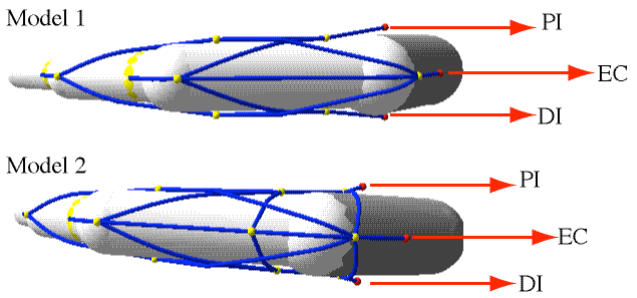
As an example, we present simulations of two alternative topologies of the extensor mechanism of a generic index finger to demonstrate how the choice of topology affects the transmission of tendon tension. While this conjecture has been mentioned in the literature (e.g., [4, 14]), this study is the first to directly and quantitatively compare two alternative 3D topologies of the extensor mechanism. To emphasize the effect of topology, i) all compliant tendinous elements were assigned the same nominal stiffness, ii) the phalanges were fixed in space in a functional posture, iii) the bony insertions of dorsal interosseous and the extensor tendon onto the proximal phalanx were not included (they vary across fingers), and iv) the lumbrical muscle was not included (its insertion varies across fingers, and has its origin in the deep flexor which is not part of the extensor mechanism). Model 1 corresponds to Winslow's tendinous rhombus (dating from the 17th century), and Model 2 was proposed by Garcia-Elias [4] when measuring the tensile properties of the tendinous elements of the extensor mechanism. The Figure labels the nodes (yellow) of each network to define all tendinous elements (blue). Model 1 has no "B" or "I" nodes. In our results, we compared element AC in Model 1 to element BC in Model 2. They yellow dots on the middle and distal phalanges are the visible portions of the insertion node onto the bone.

We described generic extensor mechanisms for a right-hand index finger as Models 1 and 2 (see Figure). These longitudinally symmetric complex networks of tendinous elements were placed in equilibrium (using the relaxation algorithm described below) such that they would wrap over the phalanges idealized as spheres and cylinders. We applied a nominal anatomically realistic 25N tension to the input tendons EC (extensor digitorum communis), DI (dorsal interosseous) and PI (palmar interosseous) in three cases. Case I: apply tension to all three input tendons; Case II: apply tension to the interosseous tendons DI and PI; and Case III: apply tension to the extensor tendon EC. (See bottom of Table). The simulations computed the resulting tensions in all elements when the network reached equilibrium as per the relaxation algorithm described below.

III. Results

The Table lists the tension in each element of the extensor

		Element	Model 1 (N)	Model 2 (N)	% Change
Case I	Input tension	EC	25	25	
		DI	25	25	
		PI	25	25	
	Resulting tensions	AC/BC	5.4	21.8	305.0
		CD	32.2	29.2	-9.4
		EH	27.6	18.5	-32.8
		AF	10.0	5.0	-50.0
		FE	16.9	11.4	-32.6
		GC	17.3	4.7	-72.8
		GF	9.5	7.9	-17.1
Case II	Input tension	EC	0	0	
		DI	25	25	
		PI	25	25	
	Resulting tensions	AC/BC	0.0	12.7	
		CD	18.9	19.7	4.7
		EH	26.1	12.1	-53.8
		AF	3.4	1.6	-52.9
		FE	19.1	7.5	-60.9
		GC	12.5	4.2	-66.7
		GF	16.4	6.8	-58.4
Case III	Input tension	EC	25	25	
		DI	0	0	
		PI	0	0	
	Resulting tensions	AC/BC	17.8	15.6	-12.7
		CD	18.1	16.5	-8.9
		EH	5.4	5.8	7.0
		AF	4.0	4.3	8.5
		FE	3.4	3.7	9.2
		GC	0.7	1.0	35.2



mechanisms. For this symmetric example, we report only for one side; although our computational substrate can simulate asymmetric tendinous networks and asymmetric loading. Our results show that comparable elements for networks with moderate topological differences can carry very different tensions for the same nominal inputs. The effect is most pronounced for Case I where all elements are loaded, and least pronounced for Case III where, as expected, the transmission of load from the centrally located EC tendon is not affected by the extra interconnections that are perpendicular to EC line of action. Thus, the topology of the extensor mechanism is an important consideration when creating biomechanical models of the extensor mechanism. Our computational substrate will allow us to test the consequences and validity of alternative topologies by, for example, comparing against multiple loading conditions in cadaveric digits [13].

IV. Conclusions

We have created a computational environment to describe and simulate 3D biomechanical systems, like the extensor mechanism of the fingers, which contain complex tendinous networks that were not previously amenable to biomechanical simulation. We find that, all other things being equal, moderate changes in the topology of the extensor mechanism greatly affect the distribution of load through its individual elements, and will affect the biomechanical predictions of finger motion and force. We will now begin to validate this computational environment by conducting tests on synthetic and cadaveric networks using a computer-controlled system that can deliver known tensions while measuring output forces, displacements and strains [13]. This work will be instrumental to the realistic prediction of finger motion and force production for precision pinch.

Acknowledgment

This material is based upon work supported by the National Science Foundation under Grants No. 0237258 (CAREER award) and No. 0312271 (ITR project); and a Biomedical Engineering Research Grant from the Whitaker Foundation to FVC.

References

[1] Bunnell, S., *Surgery of the hand*. 1944, Philadelphia: J.B. Lippincott Co. 930.

[2] Cole, K.J. and J.H. Abbs, *Coordination of three-joint digit movements for rapid finger-thumb grasp.* J Neurophysiol, 1986. **55**(6): p. 1407-23.

[3] Dennerlein, J.T., C.D. Mote, Jr., and D.M. Rempel, *Control strategies for finger movement during touch-typing. The role of the extrinsic muscles during a keystroke.* Experimental Brain Research, 1998. **121**(1): p. 1-6.

[4] Garcia-Elias, M., K.N. An, L. Berglund, R.L. Linscheid, W.P. Cooney, and E.Y. Chao, *Extensor mechanism of the fingers: I. A quantitative geometric study.* Journal of Hand Surgery (American), 1991. **16**(6): p. 1130-40.

[5] Keen, D.A. and A.J. Fuglevand, *Role of intertendinous connections in distribution of force in the human extensor digitorum muscle.* Muscle Nerve, 2003. **28**(5): p. 614-22.

[6] Leijnse, J.N., C.J. Snijders, J.E. Bonte, J.M. Landsmeer, J.J. Kalker, J.C. Van der Meulen, G.J. Sonneveld, and S.E.R. Hovius, *The hand of the musician: kinematics of the bidigital finger system with anatomical restrictions.* Journal of Biomechanics, 1993. **26**(10): p. 1169-79.

[7] Lipson, H. and J.B. Pollack, *Automatic design and manufacture of robotic lifeforms.* Nature, 2000. **406**(6799): p. 974-8.

[8] Lipson, H., *A computational relaxation method for simulating compound nonlinear mechanisms.* ASME Journal of Mechanical Design, In review. **In review**.

[9] McAuley, J.H., J.C. Rothwell, and C.D. Marsden, *Frequency peaks of tremor, muscle vibration and electromyographic activity at 10 Hz, 20 Hz and 40 Hz during human finger muscle contraction may reflect rhythmicities of central neural firing.* Experimental Brain Research, 1997. **114**(3): p. 525-41.

[10] Murray, R.M., Z. Li, and S.S. Sastry, *A mathematical introduction to robotic manipulation*. 1994, Boca Raton: CRC Press. 456.

[11] Santello, M., M. Flanders, and J.F. Soechting, *Postural hand synergies for tool use.* J Neurosci, 1998. **18**(23): p. 10105-15.

[12] Valero-Cuevas, F.J., F.E. Zajac, and C.G. Burgar, *Large index-fingertip forces are produced by subject-independent patterns of muscle excitation.* Journal of Biomechanics, 1998. **31**(8): p. 693-703.

[13] Valero-Cuevas, F.J., J.D. Towles, and V.R. Hentz, *Quantification of fingertip force reduction in the forefinger following simulated paralysis of extensor and intrinsic muscles.* Journal of Biomechanics, 2000. **33**(12): p. 1601-09.

[14] Zancolli, E., *Structural and dynamic bases of hand surgery*. 2nd ed. 1979, Philadelphia: Lippincott. 375.

[15] Zatsiorsky, V.M., Z.M. Li, and M.L. Latash, *Coordinated force production in multi-finger tasks: finger interaction and neural network modeling.* Biol Cybern, 1998. **79**(2): p. 139-50.